Heat Transfer on MHD Convective Flow Through Porous Medium Between Two Concentric Cylinders

B.V. Swarnalathamma

Department of Science and Humanities, JB Institute of Engineering & Technology, Moinabad, Hyderabad, Telangana-500075, India. Email: bareddy_swarna@yahoo.co.in

Abstract:

This paper addresses the effect of porous medium in magnetohydrodynamic (MHD) unsteady flow of a viscous non-gray optically thin fluid between two infinite concentric vertical cylinders under the influence of time dependent periodic pressure gradient subjected to anazimuthal direction applied magnetic field. Effects of thermal radiation and periodic wall temperature are also taken into consideration. The governing non-dimensional equations are transformed into ordinary differential equations which are then solved in terms of the modified Bessel functions. The effects of various parameters on the velocity, temperature, skin friction, the rate of heat transfer at the surface of the cylinders are evaluated computationally and are discussed graphically. It is observed that velocity of the fluid increases with an increase in permeability of the porous medium. Present computations are consistent with those of existing studies in limiting sense.

Keywords: heat transfer; periodic pressure gradient; periodic wall temperature; porous medium; thermal radiation

1. Introduction:

Convection in porous media has a wide range of applications in engineering like oil and gas extraction, ground water movement, packed bed reactors, etc. Flow in a porous channel of different shapes especially parallel plates and cylindrical pipes are quite prominent and interesting in geophysics, chemical engineering, and petroleum industry etc. If the fluid is conducting fluid, the effect of magnetic field on the flow becomes important. A good amount of literature is available on flow though porous channels [1-6]

An important class of problems related to flow of electrically conducting fluid in porous medium is MHD flow. The investigation regarding the MHD flow in an annular region has fascinated the consideration of several researchers owing to its extensive demands in hydraulics and nuclear technology. Chamkha [7] studied the unsteady laminar hydromagnetic fluid-particle flow and heat transfer in channels and circular pipes. Singh [8] analyzed the exact solution of MHD mixed convection periodic flow in a rotating vertical channel with heat radiation. Krishna and Gangadhar Reddy [9] discussed the unsteady MHD free convection in a boundary layer flow of an electrically conducting fluid through porous medium subject to uniform transverse magnetic field over a moving infinite vertical plate in the presence of heat source and chemical reaction. Krishna and Subba Reddy [10] have investigated the simulation on the MHD forced convective flow through stumpy permeable porous medium (oil sands, sand) using Lattice Boltzmann method. Krishna and Jyothi [11] discussed the Hall effects on MHD Rotating flow of a visco-elastic fluid through a porous medium over an infinite oscillating porous plate with heat source and chemical reaction. Sadiq et al. [12] the steady fully developed MHD free convection flow through a porous medium in a micro-channel bounded by two infinite vertical parallel plates due to asymmetric heating of plates taking Hall and ion slip effects into account. Veera Krishna et al. [13] discussed heat and mass transfer on unsteady MHD oscillatory flow of blood through porous arteriole. Krishna et al. [19] discussed the MHD flow of an electrically conducting second-grade fluid through porous medium over a semi-infinite vertical stretching sheet. The effects of radiation and Hall current on an unsteady MHD free convective flow in a vertical channel filled with a porous medium have been studied by Veera Krishna et al. [20]. The heat generation/absorption and thermo-diffusion on an unsteady free convective MHD flow of radiating and chemically reactive second grade fluid near an infinite vertical plate through a porous medium and taking the Hall current into account have been studied by Veera Krishna and Chamkha [21]. Veera Krishna and Chamkha [22] discussed the MHD squeezing flow of a water-based nanofluid through a saturated porous medium between two parallel disks, taking the Hall current into account. Veera Krishna et al. [23] discussed Hall effects on MHD peristaltic flow of Jeffrey fluid through porous medium in a vertical stratum.

More recently, Veera Krishna and Chamkha [24] investigated The diffusion-thermo, radiation-absorption and Hall and ion slip effects on MHD free convective rotating flow of nano-fluids (Ag and TiO2) past a semi-infinite permeable moving plate with constant heat source. Veera Krishna et al.[25] discussed the Soret and Joule effects of MHD mixed convective flow of an incompressible and electrically conducting viscous fluid past an infinite vertical porous plate taking Hall effects into account. Veera Krishna and Chamkha [26] discussed the MHD squeezing flow of a water-based nanofluid through a saturated porous medium between two parallel disks, taking the Hall current into account. Hall and ion slip effects on Unsteady MHD Convective Rotating flow of Nanofluids have been discussed by Veera Krishna and Chamkha[27]. Veera Krishna [28] investigated the heat transport on steady MHD flow of copper and alumina nanofluids past a stretching porous surface. Veera Krishna et al.[29] discussed investigated the Hall and ion slip effects on the unsteady MHD free convective rotating flow through porous medium past an exponentially accelerated inclined plate. The combined effects of Hall and ion slip on MHD rotating flow of ciliary propulsion of microscopic organism through porous medium have been studied by Veera Krishna et al.[30]. Veera Krishna and Chamkha [31] investigated the Hall and ion slip effects on the MHD convective flow of elastico-viscous fluid through porous medium between two rigidly rotating parallel plates with time fluctuating sinusoidal pressure gradient. Veera Krishna [32] reported that the Hall and ion slip effects on MHD free convective rotating flow bounded by the semi-infinite vertical porous surface. Veera Krishna [33] discussed the MHD laminar flow of an elastico-viscous electrically conducting Walter's fluid through a circular cylinder or a pipe.

The main purpose of this work is to explore the effect of porous medium on a laminar unsteady MHD flow of a viscous incompressible and electrically conducting Newtonian non-gray optically thin fluid between two infinite concentric vertical cylinders.

2. Formulation and Solution of the problem:

A laminar unsteady MHD flow of a viscous incompressible and electrically conducting Newtonian non-gray optically thin fluid through porous medium between two infinite concentric vertical cylinders has been investigated. The flow influenced by time dependent periodic pressure gradient subjected to a magnetic field applied in azimuthally direction and in the presence of appreciable thermal radiation and periodic wall temperature.The governing equationsfor the flow are

$$\vec{\nabla}.\vec{q}=0 \tag{1}$$

$$\rho\left(\frac{\partial\vec{q}}{\partial t}+(\vec{q}.\vec{\nabla})\vec{q}\right)=-\vec{\nabla}p+\mu\nabla^2\vec{q}+\vec{J}\times\vec{B}+\rho\vec{g} \tag{2}$$

$$\rho C_p\left(\frac{\partial T}{\partial t}+(\vec{q}.\vec{\nabla})T\right)=K_T\nabla^2 T+\varphi-\vec{\nabla}.\vec{q}_r \tag{3}$$

Ohm's law for an electrically conducting fluid:

$$\vec{J}=\sigma\left(\vec{q}\times\vec{B}\right) \tag{4}$$

The annulus is assumed to be bounded by two cylinders of radii a and b, where $a<b$. A

cylindrical polar coordinate system (r, θ, z) is introduced with the axis of the coaxial cylinders as the z-axis. A magnetic field of intensity H_0 (constant) is applied in the azimuthal direction (Fig.1).All the fluid properties are considered constants except the influence of the variation in density in the buoyancy force term and neglecting viscous dissipation. The radiation heat flux (q_r) in the vertical direction is considered to be negligible in contrast to that in the normal direction.

We recall that the fluid moves parallel to the z-axis, $\vec{q}$ as $(0,0,V_z)$. Equation (1) in (r,θ,z) system becomes $\frac{1}{r}\frac{\partial}{\partial t}(rV_z)=0$, which yields $V_z = V_z(r,t)$, by symmetry. The momentum equation takes the form

$$\rho\frac{\partial V_z}{\partial t}=-\frac{\partial p}{\partial z}+\mu\left(\frac{\partial^2 V_z}{\partial r^2}+\frac{1}{r}\frac{\partial V_z}{\partial r}\right)-\sigma\mu_e^2H_0^2V_z-\rho g-\frac{\mu}{\rho k}V_z \quad (5)$$

The equation of state on the basis of classical Boussinesq approximation (Bergman *et al.* [14]) is

$$\rho_s \approx \rho\left[1+\beta\left(T-T_s\right)\right] \quad (6)$$

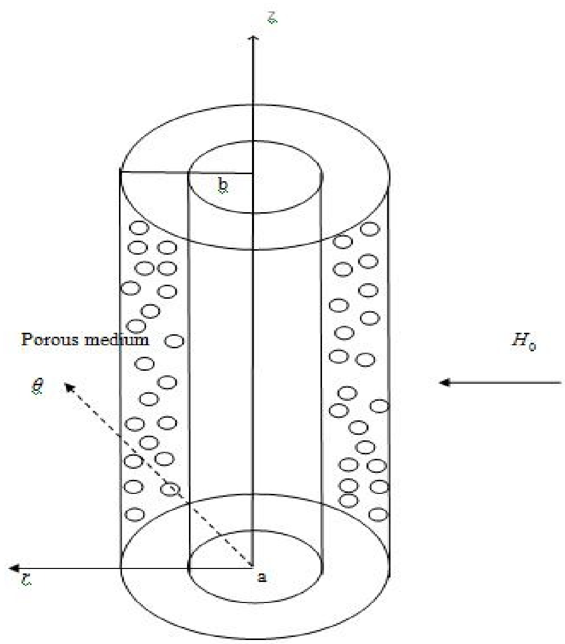

Fig. 1 Physical Configuration of the Problem

In the static condition, (5) renders $0=-\frac{\partial p_s}{\partial z}-\rho_s g$. Utilization of this in (5) produces

$$\rho\frac{\partial V_z}{\partial t}=-\frac{\partial\left(p-p_s\right)}{\partial z}+\mu\left(\frac{\partial^2 V_z}{\partial r^2}+\frac{1}{r}\frac{\partial V_z}{\partial r}\right)-\sigma\mu_e^2H_0^2V_z-\frac{\mu}{\rho k}V_z-g\left(\rho-\rho_s\right) \quad (7)$$

With $P = p - p_s$,the application of (6) leads to the following equation of motion:

$$\frac{\partial V_z}{\partial t}=-\frac{1}{\rho}\frac{\partial P}{\partial z}+\frac{\mu}{\rho}\left(\frac{\partial^2 V_z}{\partial r^2}+\frac{1}{r}\frac{\partial V_z}{\partial r}\right)-\frac{\sigma\mu_e^2H_0^2}{\rho}V_z-\frac{\nu}{k}V_z+g\beta\left(T-T_s\right) \quad (8)$$

In lieu of the assumptions (2) and (3), the energy equation takes the form

$$\rho C_p\frac{\partial T}{\partial t}=K_T\left(\frac{\partial^2 T}{\partial r^2}+\frac{1}{r}\frac{\partial T}{\partial r}\right)-4I\left(T-T_s\right) \quad (9)$$

The annulus being infinite in the z-direction with the axial symmetry, thetemperature field is independent of θ and z. In (9), the rate of radiative heat flux in the optically thin limit for a non-gray gas near equilibrium is,

$$\frac{\partial q_r}{\partial r}=4I\left(T-T_s\right) \quad (10)$$

Where $I=\int_0^\infty\left(K_{\lambda^*}\right)_w\left(\frac{\partial e_{\lambda^*}h}{\partial T}\right)_w d\lambda^*$

The boundary conditions are

$$\left.\begin{aligned}&V_z=0 \quad \text{at} \quad r=a;\ V_z=0 \quad \text{at} \quad r=b\\&T=T_s+T_sn_1e^{i\alpha_1 t} \quad \text{at} \quad r=a\\&T=T_s+T_sn_2e^{i\alpha_1 t} \quad \text{at} \quad r=b\end{aligned}\right\} \quad (11)$$

The following non-dimensional quantities are introduced in order to normalize the model:

$$\begin{aligned}&V_z^*=\frac{V_za}{\nu},r^*=\frac{r}{a},z^*=\frac{z}{a},P^*=\frac{Pa^2}{\mu\nu},t^*=\frac{t\nu}{a^2},\lambda=\frac{b}{a},\psi^*=\frac{T-T_s}{T_s}\\&M=\mu_eH_0a\sqrt{\frac{\sigma}{\mu}},\ K=\frac{k}{a^2},\ \mathrm{Gr}=\frac{g\beta a^3}{\nu^2}T_s,\ \mathrm{Pr}=\frac{\mu C_p}{K_T},\ Q=\frac{4la^2}{\mu C_p}\end{aligned} \quad (12)$$

The governing dimensionless forms of equations (8),(9) and the boundary conditions (11) are (Dropping asterisks):

$$\frac{\partial V_z}{\partial t}=-\frac{\partial P}{\partial z}+\left(\frac{\partial^2 V_z}{\partial r^2}+\frac{1}{r}\frac{\partial V_z}{\partial r}\right)-\left(M^2+\frac{1}{K}\right)-\mathrm{Gr}\psi \quad (13)$$

$$\mathrm{Pr}\frac{\partial \psi}{\partial t}=\frac{\partial^2\psi}{\partial r^2}+\frac{1}{r}\frac{\partial\psi}{\partial r}-Q\,\mathrm{Pr}\,\psi \quad (14)$$

$$\left.\begin{array}{l} V_z = 0 \quad \text{at} \quad r = 1;\ V_z = 0 \quad \text{at} \quad r = \lambda \\ \psi = n_1 e^{i\alpha t} \quad \text{at} \quad r = 1 \\ \psi = n_2 e^{i\alpha_1 t} \quad \text{at} \quad r = \lambda \end{array}\right\} \tag{15}$$

We consider the temperature as $\psi(r,t) = f(r)e^{i\alpha t}$ with this form of ψ the equation (14) reduces to the ordinary differential equation $r^2\frac{d^2 f(r)}{dr^2} + r\frac{df(r)}{dr} - \eta^2 r^2 f(r) = 0$

Where, $\eta^2 = \Pr(i\alpha + Q)$.

The substitution $z = ir\eta,\ f\left(\frac{z}{i\eta}\right) = f_1(z)$, leads us to Bessel's differential equation of order zero.

$$z^2\frac{d^2 f_1(z)}{d^2 z^2} + z\frac{df_1(z)}{dz^2} + z^2 f_1(z) = 0 \tag{16}$$

The general solution to (16) is $f(r) = A_1 J_0(ir\eta) + B_1 Y_0(ir\eta)$, and we obtain,

$$\psi(r,t) = \left(A_1 I_0(r\eta) + B_1\left\{-\frac{2}{\pi}K_0(r\eta) - \frac{1}{i}I_0(r\eta)\right\}\right) e^{i\alpha t} \tag{17}$$

Where A_1 and B_1 are defined as

$$A_1 = \frac{\frac{2}{\pi}\{n_2 K_0(\eta) - n_1 K_0(\lambda\eta)\} + \frac{1}{i}\{n_2 I_0(\eta) - n_1 I_0(\lambda\eta)\}}{\frac{2}{\pi}\{I_0(\lambda\eta)K_0(\eta) - I_0(\eta)K_0(\lambda\eta)\}}$$

$$B_1 = \frac{n_2 I_0(\eta) - n_1 I_0(\lambda\eta)}{\frac{2}{\pi}\{I_0(\lambda\eta)K_0(\eta) - I_0(\eta)K_0(\lambda\eta)\}}$$

Assuming that the pressure gradient is a periodic of t, we formulate

$$-\frac{\partial P}{\partial z} = P_0 e^{i\alpha t}, \tag{18}$$

We consider the velocity to be $V_z(r,t) = g(r)e^{i\alpha t}$.

All these considerations in (13) finally present us with the following expression for the velocity field:

$$V_z(r,t) = \left(\frac{P_0}{\delta^2} + A_2 I_0(r\delta) + B_2\left\{-\frac{2}{\pi}K_0(r\delta) - \frac{1}{i}I_0(r\delta)\right\} + \right.$$

$$\frac{1}{\delta^2-\eta^2}\times\left\{\left(\mathrm{Gr}A_1+\mathrm{Gr}B_1\frac{1}{i}\right)I_0\left(r\eta\right)+\frac{2\mathrm{Gr}B_1}{\pi}K_0\left(r\eta\right)\right\}\Bigg)e^{i\alpha t} \quad (19)$$

With A_2 and B_2 in the form

$$A_2=\frac{1}{\frac{2}{\pi}\left\{I_0(\lambda\delta)K_0(\delta)-I_0(\delta)K_0(\lambda\delta)\right\}}\times\left(\frac{P_0}{\delta^2}\frac{2}{\pi}\left\{K_0(\lambda\delta)-K_0(\delta)\right\}+\right.$$

$$\frac{P_0}{\delta^2}\frac{1}{\pi}\left\{I_0(\lambda\delta)-I_0(\delta)\right\}+\frac{1}{\delta^2-\eta^2}\left(\mathrm{Gr}A_1+\mathrm{Gr}B_1\frac{1}{i}\right)$$

$$\left\{\frac{2}{\pi}\right\}\times\left\{I_0(\eta)K_0(\lambda\delta)-I_0(\lambda\eta)K_0(\delta)\right\}+\frac{1}{\delta^2-\eta^2}\left(\mathrm{Gr}A_1+\mathrm{Gr}B_1\frac{1}{i}\right)$$

$$\frac{1}{i}\times\left\{I_0(\eta)I_0(\lambda\delta)-I_0(\lambda\eta)I_0(\delta)\right\}+\frac{4\mathrm{Gr}B_1}{\delta^2-\eta^2}\frac{1}{\pi^2}$$

$$\left.\left\{K_0(\eta)K_0(\lambda\delta)-K_0(\lambda\eta)K_0(\delta)\right\}+\frac{2\mathrm{Gr}B_1}{\delta^2-\eta^2}\frac{1}{\pi i}\left\{K_0(\eta)I_0(\lambda\delta)-K_0(\lambda\eta)I_0(\delta)\right\}\right)$$

$$B_2=\frac{1}{\frac{2}{\pi}\left[I_0(\lambda\delta)K_0(\delta)-I_0(\delta)K_0(\lambda\delta)\right]}\times\left(\frac{P_0}{\delta^2}\left\{I_0(\lambda\delta)-I_0(\delta)\right\}+\frac{1}{\delta^2-\eta^2}\left(\mathrm{Gr}A_1+\mathrm{Gr}B_1\frac{1}{i}\right)\right.$$

$$\left.\times\left\{I_0(\eta)I_0(\lambda\delta)-I_0(\lambda\eta)I_0(\delta)\right\}+\frac{2\mathrm{Gr}B_1}{\delta^2-\eta^2}\frac{1}{\pi i}\left\{K_0(\eta)I_0(\lambda\delta)-K_0(\lambda\eta)I_0(\delta)\right\}\right)$$

Where,

$$\delta^2=M^2+\frac{1}{K}+i\alpha$$

The viscous drags per unit area on the surface of the inner cylinder and outer cylinder, respectively, are specified by Newton's law of viscosity as mentioned below:

$$\tau_1=-\mu\left.\frac{\partial V_z}{\partial r}\right|_{r=a} \text{ and } \tau_2=-\mu\left.\frac{\partial V_z}{\partial r}\right|_{r=b} \quad (20)$$

The non dimensional forms of (20) are

$$\tau_1=-\frac{\mu\nu}{a^2}\left.\frac{\partial V_z^*}{\partial r^*}\right|_{r^*=1} \quad \text{and} \quad \tau_2=-\frac{\mu\nu}{a^2}\left.\frac{\partial V_z^*}{\partial r^*}\right|_{r^*=\lambda} \quad (21)$$

The coefficient of the skin friction on the surface of the inner and outer cylinders are respectively, specified by

$$C_{f1}=\frac{\tau_1}{\frac{\mu\nu}{a^2}}=-\frac{\partial V_z}{\partial r}\Big|_{r=1}=-\Bigg[\delta\left\{A_2I_{-1}(\delta)+\frac{2B_2}{\pi}K_{-1}(\delta)-\frac{B_2}{i}I_{-1}(\delta)\right\}$$

$$+\frac{1}{\delta^2-\eta^2}\left(\text{Gr}A_1+\text{Gr}B_1\frac{1}{i}\right)\eta I_{-1}(\eta)-\frac{1}{\delta^2-\eta^2}\frac{2\eta\text{Gr}B_1}{\pi}K_{-1}(\eta)\Bigg]e^{i\alpha t} \quad (22)$$

$$C_{f2}=\frac{\tau_2}{\frac{\mu\nu}{a^2}}=-\frac{\partial V_z}{\partial r}\Big|_{r=\lambda}=-\Bigg[\delta\left\{A_2I_{-1}(\lambda\delta)+\frac{2B_2}{\pi}K_{-1}(\lambda\delta)-\frac{B_2}{i}I_{-1}(\lambda\delta)\right\}+$$

$$\frac{1}{\delta^2-\eta^2}\left(\text{Gr}A_1+\text{Gr}B_1\frac{1}{i}\right)\times\eta I_{-1}(\lambda\eta)-\frac{1}{\delta^2-\eta^2}\frac{2\eta\text{Gr}B_1}{\pi}K_{-1}(\lambda\eta)\Bigg] \quad (23)$$

The heat fluxes q^* from the surface of the inner and outer cylinders are

$$q_1^*=-K_T\frac{\partial T}{\partial r}\Big|_{r=a} \text{ and } q_2^*=-K_T\frac{\partial T}{\partial r}\Big|_{r=b} \quad (24)$$

Using non-dimensional quantities defined, as in (12), we deduce

$$q_1^*=-\frac{K_TT_s}{a}\frac{\partial\psi^*}{\partial r^*}\Big|_{r^*=1} \text{ and } q_2^*=-\frac{K_TT_s}{a}\frac{\partial\psi^*}{\partial r^*}\Big|_{r^*=\lambda} \quad (25)$$

The coefficients of heat transfer (Nusselt number) on the surface of the inner and outer cylinder are,

$$Nu_1=\frac{q_1^*a}{K_TT_s}=-\frac{\partial\psi}{\partial r}\Big|_{r=1}=-\left[A_1\eta I_{-1}(\eta)-B_1\eta\left\{\frac{2}{\pi}K_{-1}(\eta)-\frac{1}{i}I_{-1}(\eta)\right\}\right]e^{i\alpha t} \quad (26)$$

$$Nu_2=\frac{q_2^*a}{K_TT_s}=-\frac{\partial\psi}{\partial r}\Big|_{r=\lambda}=-\left[A_1\eta I_{-1}(\lambda\eta)-B_1\eta\left\{\frac{2}{\pi}K_{-1}(\lambda\eta)-\frac{1}{i}I_{-1}(\lambda\eta)\right\}\right]e^{i\alpha t} \quad (27)$$

The total discharge of flux (mass flux) per unit time is give

$$M_f=\int_0^{2\pi}\int_1^{\lambda}V_z r\,dr\,d\theta=2\pi e^{i\alpha t}\Bigg[\left(A_2-\frac{B_2}{i}\right)\frac{1}{\delta}\left\{\lambda I_1(\lambda\delta)-I_1(\delta)\right\}-\frac{2B_2}{\pi\delta}\left\{K_1(\delta)-\lambda K_1(\lambda\delta)\right\}$$

$$+\frac{P_0}{\delta^2}\frac{1}{2}\left(\lambda^2-1\right)+\frac{1}{\delta^2-\eta^2}\frac{1}{\eta}\Bigg\{\left(\text{Gr}A_1+\text{Gr}B_1\frac{1}{i}\right)\left\{\lambda I_1(\lambda\eta)-I_1(\eta)\right\}$$

$$+\frac{2\text{Gr}B_1}{\pi}\left\{K_1(\eta)-\lambda K_1(\lambda\eta)\right\}\Bigg\}\Bigg] \quad (28)$$

3. Results and Discussion:

In order to have a clear insight of the physical problem, it is imperative to carry out numerical computations from the analytical solutions for the velocity field, temperature field, the mass flux coefficient, the coefficient of skin friction, and the Nusselt number by assigning some arbitrarily chosen specific values to the physical parameters like the Hartmann number *M*, Prandtl number Pr, radiation parameter *Q*, Grashof number Gr, the frequency parameter α and time *t*, and the results are presented in Figures 2 to 24. In most of the cases of our investigation, the value of the Prandtl number Pr is chosen to be 0.025 which corresponds to mercury at 20°C and at 1 atmospheric pressure. In Table 1, Pr is specified to be 0.71, which represents air at 20°C and at 1 atmospheric pressure. Figures 2 to 7 demonstrate the velocity profiles under the influence of *M*, *K*, *Q*, Gr, Pr and α respectively.

We noticed from the Fig. 2, an increase in the Hartmann number *M* reasons retardation to the fluid flow, the imposition of the azimuthal magnetic field decelerates the flow and therefore the thickness of the velocity boundary layer diminished due to Lorentz force. The velocity enhances with increasing the permeability of the porous medium throughout the fluid region (Fig. 3). Hence, lower the permeability lesser the fluid speed is observed in the cylinder. The radiation parameter *Q* registers the effect of thermal radiation. Retardation in fluid flow under the effect of thermal radiation is envisaged in Fig.4. The fluid velocity is inhibited substantially, since thermal radiation grades in a drop in thermal energy and the physics of this situation designate a loss in kinetic energy of the fluid.Fig.5depicts that buoyancy force origins the fluid flow to hasten. Fig. 6shows an increase in Pr, reduce in thermal diffusivity, low thermal diffusivity leads to a corresponding reduce in the kinetic energy, which affects the fluid velocity disagreeably. We noticed from the Fig. 7 that the magnitude of the velocity reduces with increasing frequency parameter α throughout the fluid region.Figs.8 to10 describe the influence of α, Pr, and *Q* on the temperature. Fig.8 suggests that the temperature can be diminished with frequency parameter. Fig.9depicts the reducing fluid temperature and is directly proportional to the diminution in thermal diffusivity. Fig.10 the fluid temperature get lowered with an increasing dissipation of thermal energy caused due to thermal radiation. From the Figs. 11 and 15 the magnitude of the skin friction reduces with increasing *M* being the other parameters fixed. This has been observed in the entire inner and outer walls of the cylinder. It is evident from the Figs 12 and 16 that the skin friction enhances initially and then gradually decreases inner walls of the cylinder with increasing permeability. The similar behaviour is observed at the outer wall of the cylinder. The effect of thermal radiation parameter is highly unpronounced on the friction at both walls of the annulus (Figure 13 and 17). The magnitude of the skin friction is boost up with increasing Grashof number Gr at both wall of the cylinder (Fig. 14 & 18). Figs.20 &22 depict that an increase in Gr or K results in the mass flux to increase in the direction of the fluid flow and this may be attributed to the buoyancy forces acting on the fluid and also it causes the permeability. However, Figs.19, 21 & 23 show a reverse trend in mass flux direction with an increase in M, QandPr. When the frequency parameter α increases the wave length of the mass flux profile reduces in magnitude throughout the fluid region (Fig.24).

Table 1 illustrate how the rate of heat transfer from the walls to the fluid is influencedby Prand α with an increase in radiation parameter Q. As thermal diffusivityof the fluid reduced, rate of heat transfer enhances from one of the walls isevident, the thermal radiation is assumed to be constant. An enhancement of the frequency parameter leads to a comprehensive growsthin the rate of heat transfer at the walls. When air is used a completely different behaviour is marked for Nusselt number at the walls of the annulus. Hence, the fluid must be carefully selected if different rates of heat transfer are wished at theinner and the outer walls of the annulus. Table 2 Represent the comparison of the results when the parameter $K \to \infty$. We observe that, it is an excellent agreement with the results of Ahmed et al. [18].

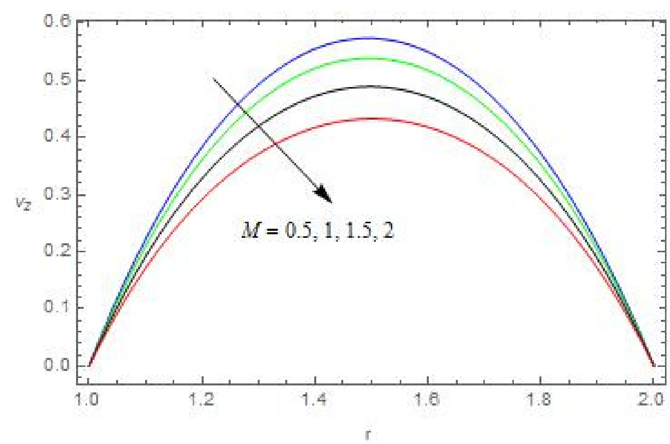

Fig.2 The velocity against M with $K = 0.5, \mathrm{Gr} = 3, \mathrm{Pr} = 0.71, Q = 2, \alpha = 0.01$

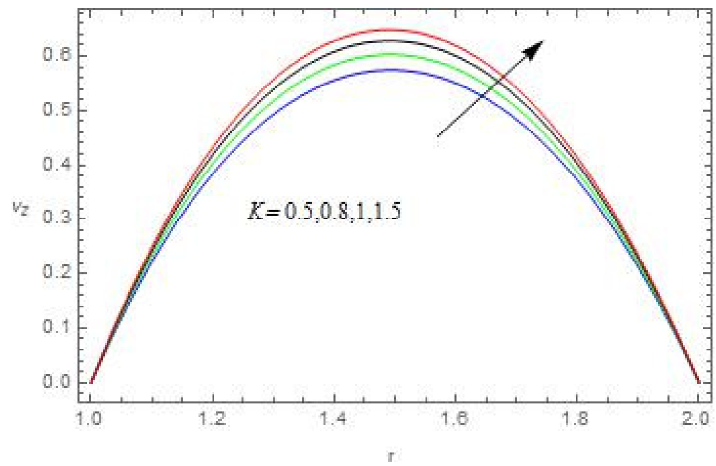

Fig.3 The velocity against K with $M = 0.5, \mathrm{Gr} = 3, \mathrm{Pr} = 0.71, Q = 2, \alpha = 0.01$

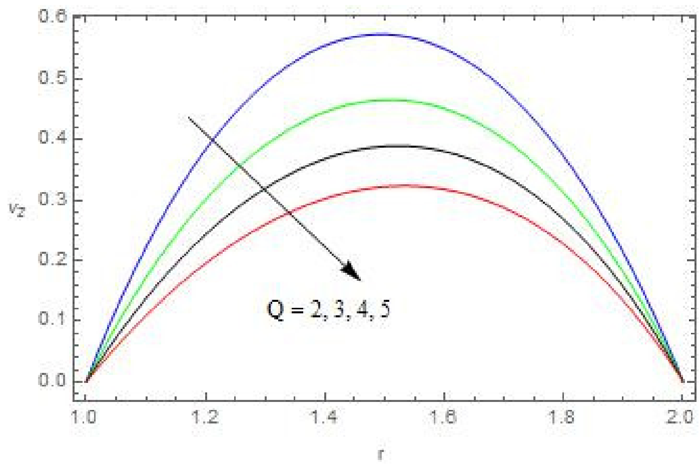

Fig.4 The velocity against Q with $M = 0.5, \mathrm{Gr} = 3, \mathrm{Pr} = 0.71, K = 0.5, \alpha = 0.01$

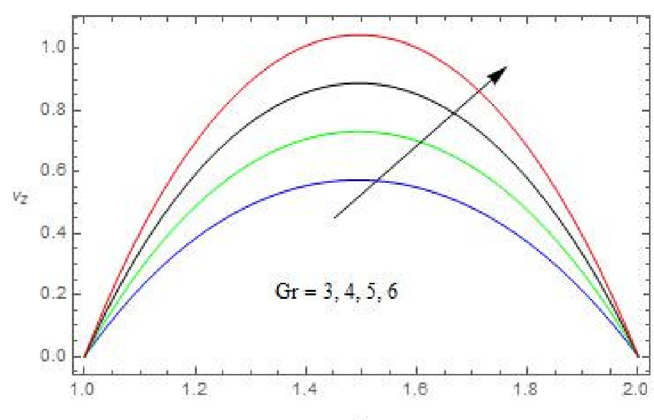

Fig.5 The velocity against Gr with $M = 0.5, K = 0.5, \mathrm{Pr} = 0.71, Q = 2, \alpha = 0.01$

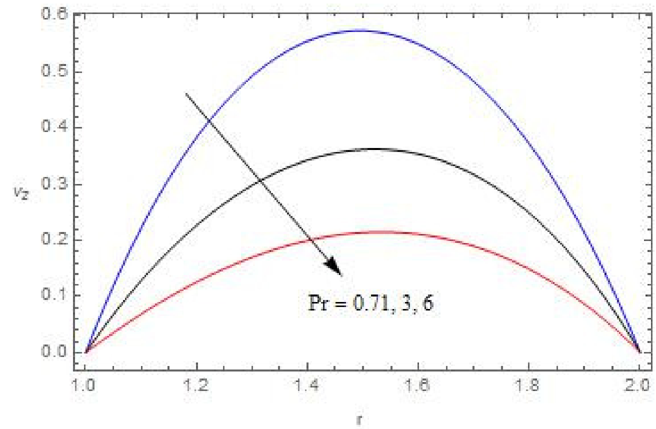

Fig.6 The velocity against Pr with $M = 0.5, K = 0.5, \mathrm{Gr} = 3, Q = 2, \alpha = 0.01$

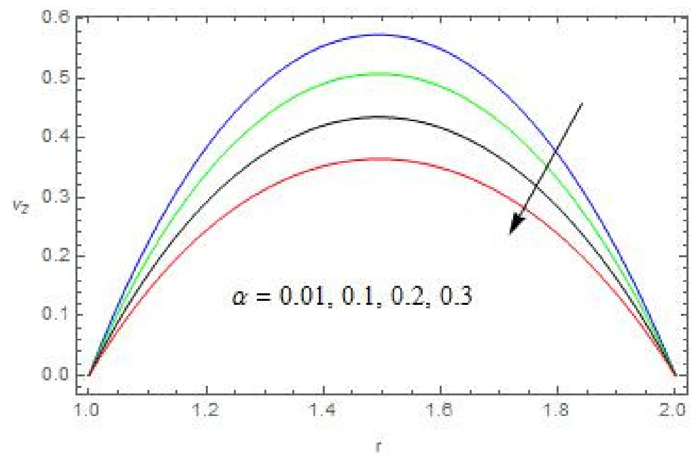

Fig.7 The velocity against α with $M = 0.5, K = 0.5, \mathrm{Gr} = 3, Q = 2, \mathrm{Pr} = 0.71$

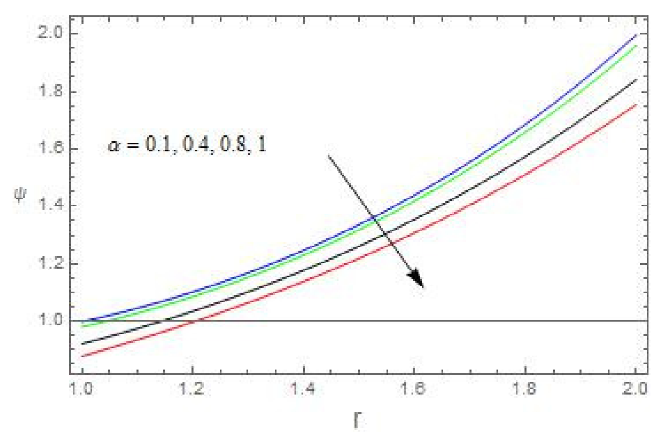

Fig.8 The Temperature Profile against α with $\mathrm{Pr} = 0.71,\ Q = 2,$

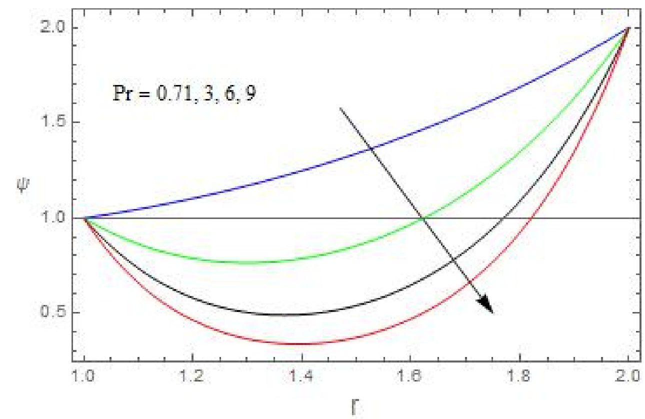

Fig.9 The Temperature Profile against Pr with $\alpha = 0.1, Q = 2,$

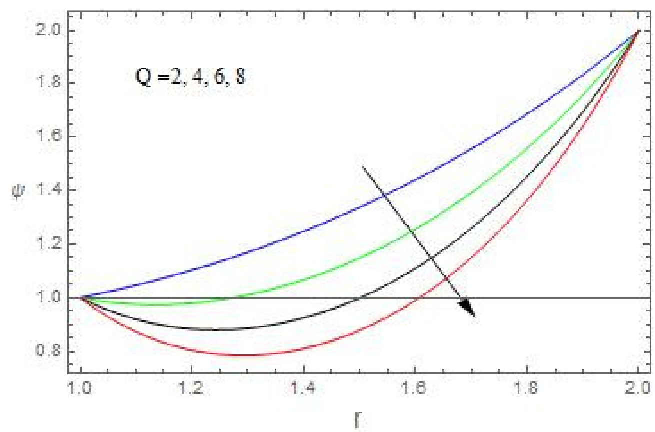

Fig.10 The Temperature Profile against Q with $\Pr = 0.71, \alpha = 0.1,$

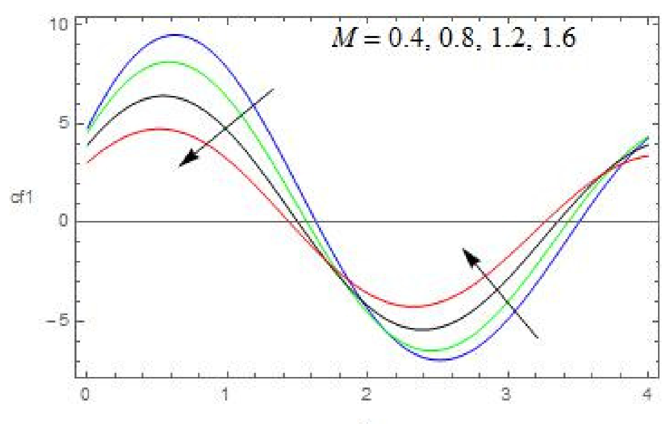

Fig.11 The Skin friction (inner wall) against M with $K = 1,, Q = 5, \mathrm{Gr} = 3.$

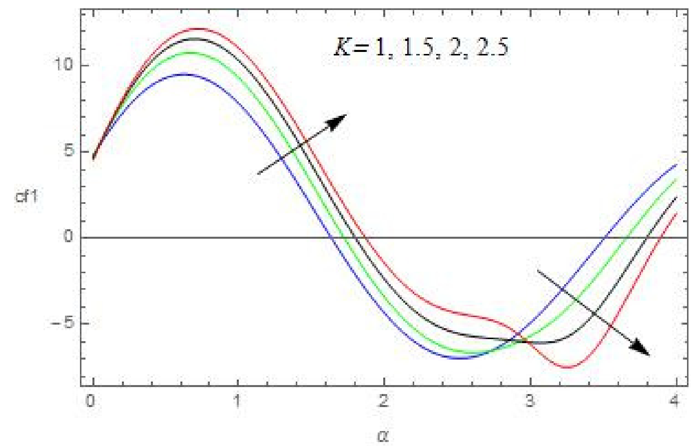

Fig.12 The Skin friction (inner wall) against K with $M = 0.4, Q = 5, \mathrm{Gr} = 3$.

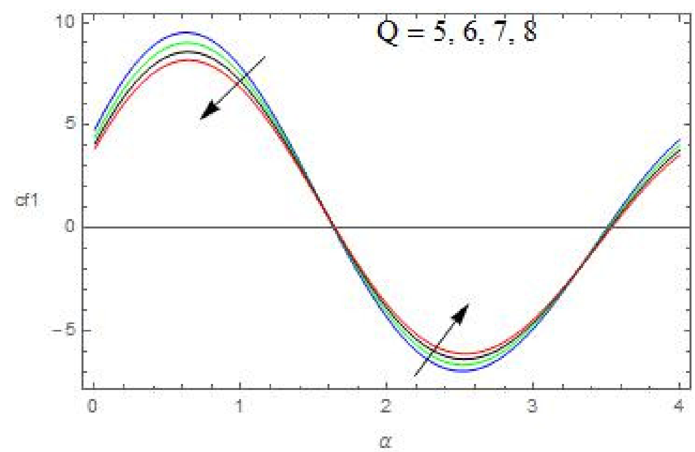

Fig.13 The Skin friction (inner wall) against Q with $M = 0.4, K = 1,, Q = 5, \mathrm{Gr} = 3$

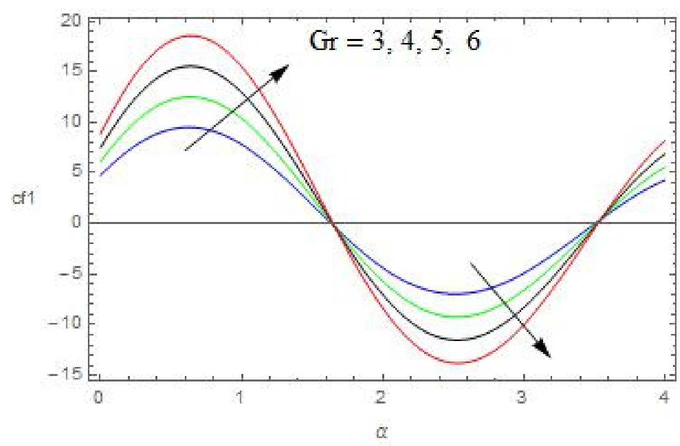

Fig.14 The Skin friction (inner wall) against Gr with $M = 0.4, K = 1,, Q = 5,$

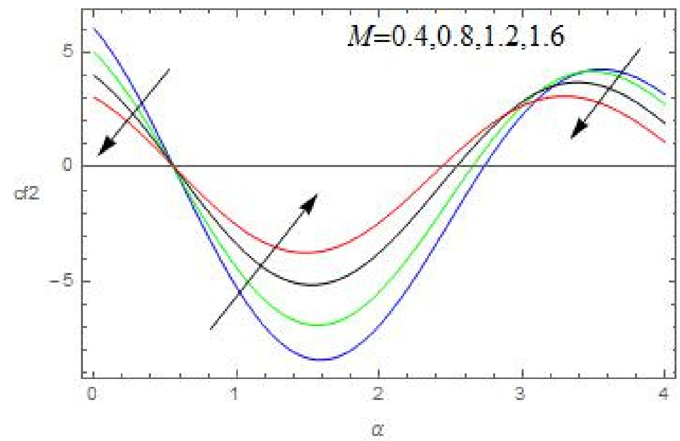

Fig.15 The Skin friction (outer wall) against M with $K = 1,, Q = 5, \mathrm{Gr} = 3.$

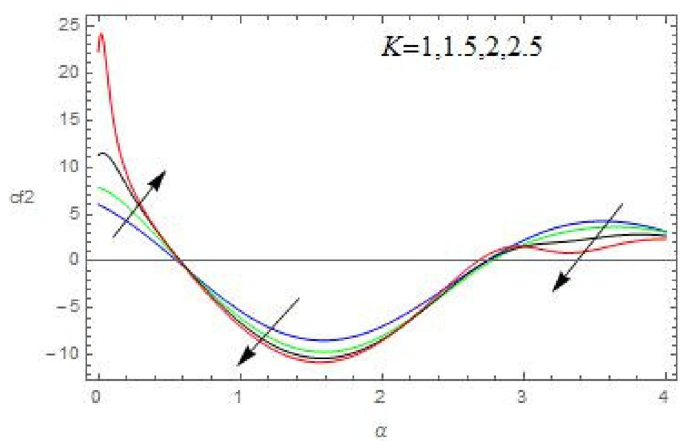

Fig.16 The Skin friction (outer wall) against K with $M = 0.4, Q = 5, \mathrm{Gr} = 3.$

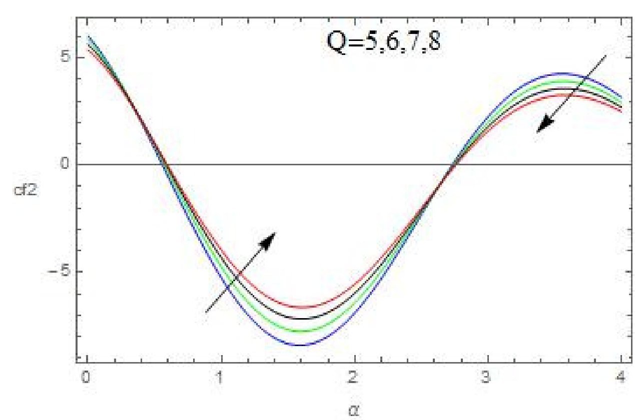

Fig.17 The Skin friction (outer wall) against Q with $M = 0.4, K = 1, \mathrm{Gr} = 3$

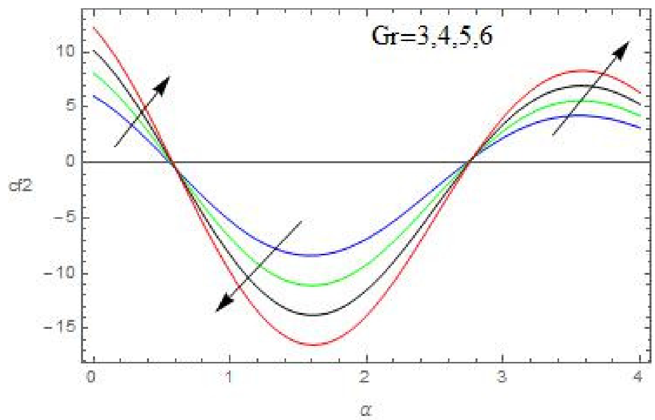

Fig.18 The Skin friction (outer wall) against Gr with $M = 0.4, K = 1,, Q = 5,$

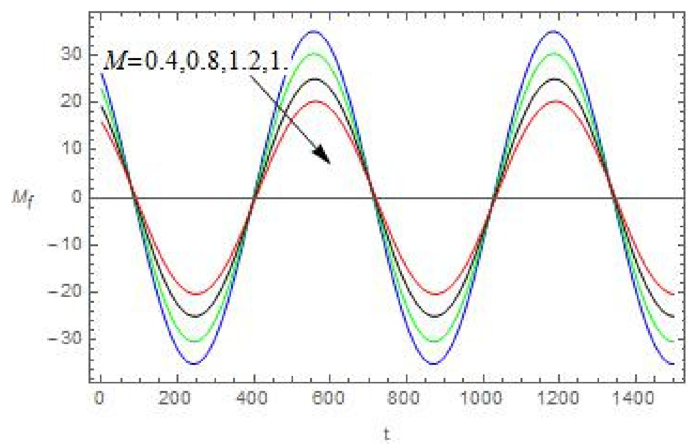

Fig.19 The Massflux against M with $\Pr = 0.025, K = 0.5, \mathrm{Gr} = 3, Q = 5, \alpha = 0.01$

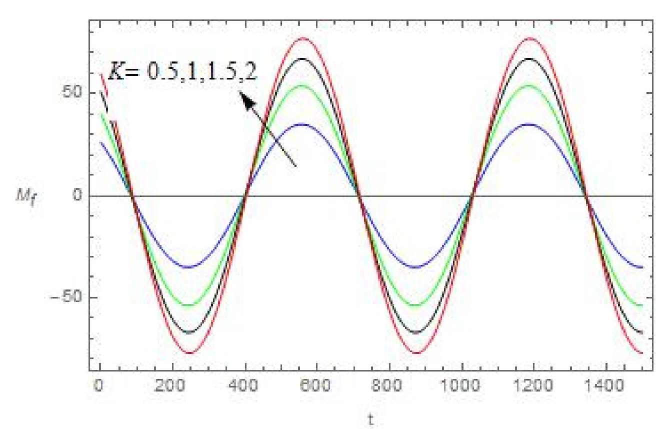

Fig.20 The Massflux against K with $\Pr = 0.025, M = 0.4, \mathrm{Gr} = 3, Q = 5, \alpha = 0.01$

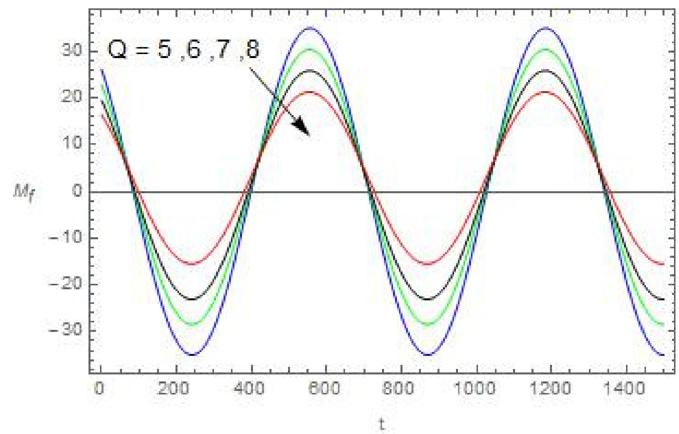

Fig.21 The Massflux against Q with $\mathrm{Pr} = 0.025, K = 0.5, \mathrm{Gr} = 3, M = 0.4, \alpha = 0.01$

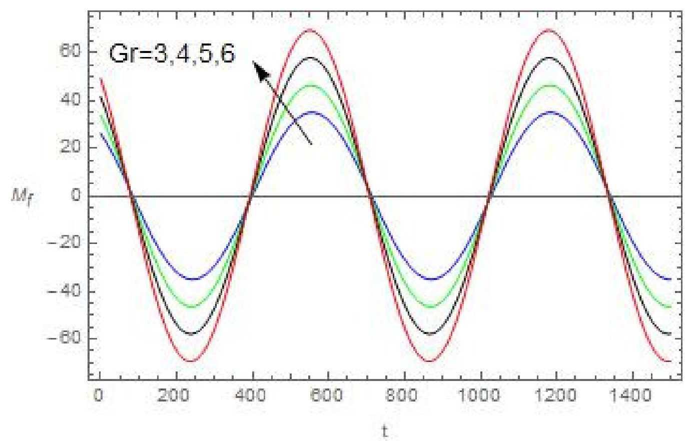

Fig.22 The Massflux against Gr with $\mathrm{Pr} = 0.025, K = 0.5, M = 0.4, Q = 5, \alpha = 0.01$

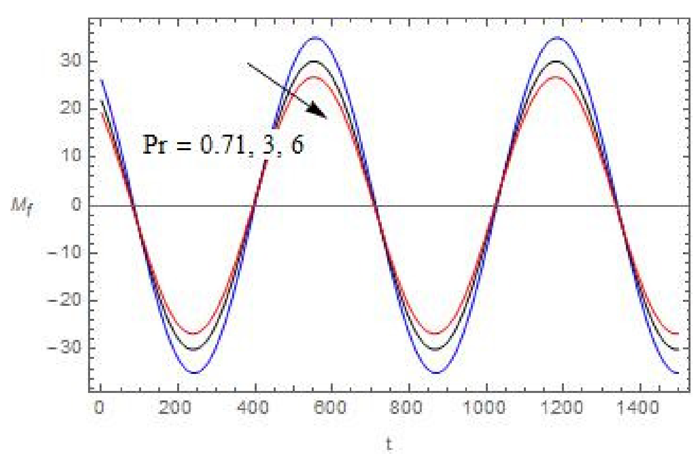

Fig.23 The Massflux against Pr with $M = 0.4, K = 0.5, \mathrm{Gr} = 3, Q = 5, \alpha = 0.01$

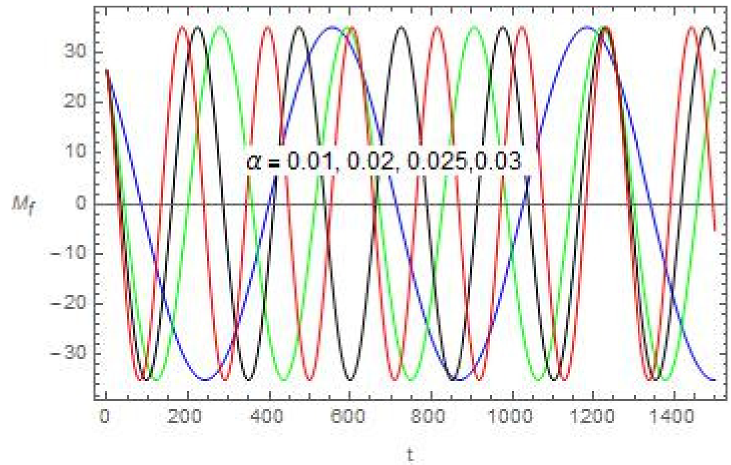

Fig.24 The Massflux against α with $\Pr = 0.025, K = 0.5, \mathrm{Gr} = 3, Q = 5, M = 0.4$

Table. 1 Nusselt number

Pr	α	Q	Nu_1	Nu_2
0.025 (Mercury)	0.01	5	1.31022	0.755768
0.050			1.2259	0.882613
0.075			1.14453	1.01203
	0.4		1.2346	0.630674
	0.6		1.17866	0.556051
		8	1.25839	0.829718
		10	1.22612	0.883162
0.71 (Air)	0.01	5	-19.2219	-99.3967
	0.4		1.2346	0.630674
	0.6		1.17866	0.556051
		8	1.25839	0.829718
		10	1.22612	0.883162

Table. 2 Comparison of Results ($n_1 = 1, n_2 = 2, t = 0.5, \lambda = 2, \alpha = 0.01, P_0 = 1$)

M	Q	Gr	Previous Results N.Ahmed et al.[22]	Present Results $K \to \infty$
0.5	2	3	0.692777	0.692776
1			0.643053	0.643052
1.5			0.574032	0.574031
	4		0.470203	0.470204
	6		0.311263	0.311262
		4	0.882709	0.882708
		5	1.07264	0.07265

4. Conclusions:

This paper deals the effect of porous medium in MHD unsteady flow of a viscous non-gray optically thin fluid between two infinite concentric vertical cylinders under the influence of time dependent periodic pressure gradient subjected to anazimuthal direction applied magnetic field. The conclusions are made as the following.

1. An amplify in the Hartmann number M causes the fluid flow to be retarded.
2. The flow reduced and therefore mass flux reduced corresponding to a reduction in the thermal diffusivity of the fluid.
3. Retardation in the fluid flow and a decrease in mass flux are observed with an increase in thermal radiation.
4. The buoyancy force causes the fluid flow to accelerate, thereby causing the mass flux to increase proportionately.
5. A reduction in fluid temperature is directly proportional to the diminution in thermal diffusivity.
6. Fluid temperature can be reduced by increasing the frequency parameter associated with the fluid flow.
7. Viscous drags at the inner and outer walls have identical magnitude but they act in opposite directions.
8. Friction at the walls increases with an increase in thermal Grashof number, but it diminishes with an increase in Prandtl number and radiation parameter, respectively.
9. The rate of heat transfer at either walls of the annulus with increasing frequency parameter depends on the Prandtl number of the fluid.

Nomenclature:

a	radius of inner cylinder
b	radius of outer cylinder
$\vec{B}$	magnetic flux density
C_{f1}	coefficient of skin friction on the surface of inner cylinder
C_{f2}	coefficient of skin friction on the surface of outer cylinder
C_p	specific heat at constantpressure
$e_{\lambda^* h}$	Planck function
$\vec{g}$	gravitational acceleration vector
g	acceleration due to gravity

$H = (0, H_0, 0)$	magnetic field vector
H_0	intensity of the applied magnetic field
i	imaginary unit
I_0	modified Besselfunction of order zero of first kind
I_1	modified Bessel function of order one of first kind
I_{-1}	modified Bessel function of order –1of first kind
$\vec{J}$	current density vector
J_0	zeroth order Bessel function of first kind
J_1	first order Bessel function of first kind
J_{-1}	Bessel function of order –1 of first kind
K_0	modified Bessel function of order 0 of second kind
K_1	modified Besselfunction of order 1 of second kind
K_{-1}	modified Bessel function of order –1 of second kind
K_T	thermal conductivity
$\left(K_{\lambda^*}\right)_w$	absorption coefficient
M	Hartmann number
M_f	mass flux per second
n_1	non-zero constant
n_2	non-zero constant
Nu_1	Nusselt number at the surface of the inner cylinder
Nu_2	Nusselt number at the surface of the outer cylinder
P	fluid pressure
p_s	fluid pressure in static condition
P_0	dimensionless pressure parameter
$q=(V_r, V_\theta, V_z)$	velocity vector
q_r	radiative heat flux
$\hat{r}$	unit vector in r-direction
r, θ, z	cylindrical polar coordinates
t	Time
T	dimensional temperature
T_s	temperature of the fluid in static condition
V_z	velocity in z-direction
Y_0	zeroth order Bessel function of second kind
Y_1	first order Bessel function of second kind
Y_{-1}	Bessel function of order –1 of second kind
$\hat{Z}$	unit vector in z-direction
Gr	Grashofnumber
Pr	Prandtl number
Q	dimensionless radiation parameter

Greek symbols:

α	dimensionless frequency parameter

α_1	dimensional frequency parameter
β	coefficient of volume expansion for heat transfer
Φ	Viscousdissipation of energy per unit volume
Ψ	non-dimensional temperature
$\hat{\theta}$	unit vector in θ –direction
λ^*	Wavelength
λ	non-dimensional parameter
μ	coefficient of viscosity
μ_e	magnetic permeability
ν	kinematic viscosity
σ	electrical conductivity
ρ	fluid density
ρ_s	density of the fluid in static condition
τ_1	viscous drag per unit area on the surface of inner cylinder
τ_2	viscous drag per unit area on the surface of outer cylinder
∇^2	Laplacian operator

References

[1]. M. Kaviany, Laminar flow through a porous channel bounded by isothermal parallel plates, Int. J. Heat Mass Transfer, vol. 28(1985), pp. 851–858.

[2]. M. Parang and M. Keyhani, Boundary effects in laminar mixed convection flow through an annular porous medium, ASME J. Heat Transfer, vol. 109(1987), pp. 1039-1041.

[3]. K. Vafai and S. J. Kim, Forced convection in a channel filled with porous medium: An exact solution, ASME J. Heat Transfer, vol. 111(1989), pp. 1103–1106.

[4]. D. A. Nield, S. L. M. Junqueira, and J. L. Lage, Forced convection in a fluid-saturated porous medium channel with isothermal or isoflux boundaries, J. Fluid Mech., vol. 322(1996), pp. 201–214.

[5]. A.Haji-Sheikh and K. Vafai, Analysis of flow and heat transfer in porous media imbedded inside various shaped ducts, Int. J. Heat Mass Transfer, vol. 47(2004), pp. 1889–1905.

[6]. B.Q. Zhao, A. Pantokratoras, T. G. Fang, and S.J. Liao, Flow of a Weakly Conducting Fluid in a Channel Filled with a Darcy-Brinkman-Forchheimer Porous Medium, Transport in Porous Media, vol. 85(2010), pp. 131–142.

[7]. Chamkha, AJ: Unsteady laminar hydromagnetic fluid-particle flow and heat transfer in channels and circular pipes. Int. J. Heat Fluid Flow 21, 740-746 (2000)

[8]. Singh, KD: Exact solution of MHD mixed convection periodic flow in a rotating vertical channel with heat radiation. Int. J. Appl. Mech. Eng. 18, 853-869 (2013)

[9]. M.Veera Krishna, M.Gangadhar Reddy, MHD Free Convective Boundary Layer Flow through Porous medium Past a Moving Vertical Plate with Heat Source and Chemical Reaction, Materials Today: Proceedings, vol. 5, pp. 91–98, (2018). https://doi.org/10.1016/j.matpr.2017.11.058.

[10]. M.Veera Krishna, G.Subba Reddy, MHD Forced Convective flow of Non-Newtonian fluid through Stumpy Permeable Porous medium, Materials Today: Proceedings, vol. 5, pp. 175–183(2018). https://doi.org/10.1016/j.matpr.2017.11.069.

[11]. M.Veera Krishna, KambojiJyotghi, Hall effects on MHD Rotating flow of a Visco-elastic Fluid through a Porous medium Over an Infinite Oscillating Porous Plate with Heat source and Chemical reaction, Materials Today: Proceedings, vol. 5, pp. 367–380, (2018).https://doi.org/10.1016/j.matpr.2017.11.094.

[12]. Sadiq Basha, P.M., Krishna M.V, Nagarathna, N., Hall and ion slip effects on steady MHD free convective flow through a porous medium in a vertical microchannel. Heat Transfer. 2020;1–17. https://doi.org/10.1002/htj.21826

[13]. VeeraKrishna.M., B.V.Swarnalathamma and J. Prakash, "Heat and mass transfer on unsteady MHD Oscillatory flow of blood through porous arteriole, Applications of Fluid Dynamics, Lecture Notes in Mechanical Engineering, vol. XXII, pp. 207-224(2018). Doi: 10.1007/978-981-10-5329-0_14.

[14]. Bergman, TL, Lavine, AS, Incropera, FP, Dewitt, DP: Fundamentals of Heat and Mass Transfer, pp. 597-598. Wiley, New York (2011)

[15]. Cogley, AC, Gilles, SE, Vincenti, WG, Ishimoto, S: Differential approximation for radiative heat transfer in a non-Gray gas near equilibrium. AIAA J. 6, 551-553 (1968).

[16]. Messiha, SAS: Laminar boundary layers in oscillatory flow along an infinite flat plate with variable suction. Math. Proc. Camb. Philos. Soc. 62, 329-337 (1966)

[17]. Vajravelu, K, Sastri, KS: Free convective heat transfer in a viscous incompressible fluid confined between a long vertical wavy wall and a parallel flat wall. J. Fluid Mech. 86, 365-383 (1978).

[18]. Nazibuddin Ahmed, Manas Dutta, Heat transfer in an unsteady MHD flow through an infinite annulus with radiation, Boundary value problems, 11, pp. 2-17(2015). DOI :10.1186/s13661-014-0279-z .

[19]. Krishna, M.V., Jyothi, K., Chamkha, A.J., Heat and mass transfer on MHD flow of second-grade fluid through porous medium over a semi-infinite vertical stretching sheet, Journal of Porous media, 23(8), pp. 751-765, 2020.

[20]. Veera Krishna.M, G.Subba Reddy, A.J.Chamkha, Hall effects on unsteady MHD oscillatory free convective flow of second grade fluid through porous medium between two vertical plates, Physics of Fluids, **30**, 023106 (2018); doi: 10.1063/1.5010863

[21]. Veera Krishna.M, A.J.Chamkha, Hall effects on unsteady MHD flow of second grade fluid through porous medium with ramped wall temperature and ramped surface concentration, Physics of Fluids, **30**, 053101 (2018); doi: 10.1063/1.5025542.

[22]. Veera Krishna.M, Ali J. Chamkha, Hall effects on MHD Squeezing flow of a water based nano fluid between two parallel disks, *Journal of porous media*, 22(2), pp. 209-223, 2019. **DOI:** 10.1615/JPorMedia.2018028721.

[23]. M. Veera Krishna, K.Bharathi, Ali.J.Chamkha, Hall effects on MHD peristaltic flow of Jeffrey fluid through porous medium in a vertical stratum, *Interfacial Phenomena and Heat transfer*, 6(3), pp. 253-268, 2019.
DOI: 10.1615/InterfacPhenomHeatTransfer.2019030215

[24]. Veera Krishna, M., Chamkha, A.J., Hall and ion slip effects on MHD rotating boundary layer flow of nanofluid past an infinite vertical plate embedded in a porous medium, Results in Physics, 15, 102652, 2019. DOI: https://doi.org/10.1016/j.rinp.2019.102652

[25]. Veera Krishna, M., Swarnalathamma, B.V., Chamkha, A.J., Investigations of Soret, Joule and Hall effects on MHD rotating mixed convective flow past an infinite vertical porous plate, Journal of Ocean Engineering and Science, 4(3), pp. 263-275, 2019. DOI: https://doi.org/10.1016/j.joes.2019.05.002.

[26]. Veera Krishna.M., Chamkha, A.J., Hall effects on MHD Squeezing flow of a water based nano fluid between two parallel disks, Journal of Porous media, 22(2), pp. 209-223, 2019. **DOI:** https://doi.org/10.1615/JPorMedia.2018028721

[27]. Veera Krishna. M., Chamkha, A.J., Hall and ion slip effects on Unsteady MHD Convective Rotating flow of Nanofluids - Application in Biomedical Engineering, Journal of Egyptian Mathematical Society, 28(1), pp. 1-14, 2020.
https://doi.org/10.1186/s42787-019-0065-2

[28]. Veera Krishna.M., Heat transport on steady MHD flow of copper and alumina nanofluids past a stretching porous surface, Heat Transfer, 49(3), 1374-1385, 2020,
doi: https://doi.org/10.1002/htj.21667

[29]. Veera Krishna, M., Ameer Ahamad, N., Chamkha, A.J., Hall and ion slip effects on unsteady MHD free convective rotating flow through a saturated porous medium over an exponential accelerated plate, Alexandria Engineering Journal, 59, 565-577, 2020. https://doi.org/10.1016/j.aej.2020.01.043

[30]. Veera Krishna, M., Sravanthi, C.S., Gorla, R.S.R., Hall and ion slip effects on MHD rotating flow of ciliary propulsion of microscopic organism through porous media, International Communications in Heat and Mass Transfer, 112, 104500, 2020. https://doi.org/10.1016/j.icheatmasstransfer.2020.104500

[31]. Veera Krishna, M., Chamkha, A.J., Hall and ion slip effects on MHD rotating flow of elastico-viscous fluid through porous medium, International Communications in Heat and Mass Transfer, 113, 104494, 2020. https://doi.org/10.1016/j.icheatmasstransfer.2020.104494

[32]. Veera Krishna, M., Hall and ion slip effects on MHD free convective rotating flow bounded by the semi-infinite vertical porous surface, Heat Transfer, 49(4), 1920–1938, 2020. https://doi.org/10.1002/htj.21700

[33]. Veera Krishna, M., Hall and ion slip effects on MHD laminar flow of an elastic-viscous (Walter's-B) fluid, Heat Transfer, 49(4), 2311–2329, 2020. https://doi.org/10.1002/htj.21722